Cancer Research

SOX5/6/21 Prevent Oncogene-Driven Transformation of Brain Stem Cells

Idha Kurtsdotter[1,2], Danijal Topcic[1,2], Alexandra Karlén[1,2], Bhumica Singla[1], Daniel W. Hagey[1,2], Maria Bergsland[1], Peter Siesjö[3], Monica Nistér[4], Joseph W. Carlson[4], Veronique Lefebvre[5], Oscar Persson[6], Johan Holmberg[1,2], and Jonas Muhr[1,2]

Abstract

Molecular mechanisms preventing self-renewing brain stem cells from oncogenic transformation are poorly defined. We show that the expression levels of SOX5, SOX6, and SOX21 (SOX5/6/21) transcription factors increase in stem cells of the subventricular zone (SVZ) upon oncogenic stress, whereas their expression in human glioma decreases during malignant progression. Elevated levels of SOX5/6/21 promoted SVZ cells to exit the cell cycle, whereas genetic ablation of SOX5/6/21 dramatically increased the capacity of these cells to form glioma-like tumors in an oncogene-driven mouse brain tumor model. Loss-of-function experiments revealed that SOX5/6/21 prevent detrimental hyperproliferation of oncogene expressing SVZ cells by facilitating an antiproliferative expression profile. Consistently, restoring high levels of SOX5/6/21 in human primary glioblastoma cells enabled expression of CDK inhibitors and decreased p53 protein turnover, which blocked their tumorigenic capacity through cellular senescence and apoptosis. Altogether, these results provide evidence that SOX5/6/21 play a central role in driving a tumor suppressor response in brain stem cells upon oncogenic insult. *Cancer Res; 77(18); 4985–97. ©2017 AACR.*

Introduction

Organ development and homeostasis depend on the proper balance between self-renewal and differentiation of stem cells. However, this balance can be shifted due to the susceptibility of self-renewing stem cells to oncogenic transformation, leading to uncontrolled proliferation associated with cancer. In the brain, glioblastoma multiforme (GBM) is the most prevalent and aggressive form of primary tumors in adults. Studies have shown that malignant transformation of neural stem cells (NSC) plays a significant role in GBM initiation and development. An important mechanism that prevents malignant transformation is the activation of signaling cascades that results in cell-cycle exit and the induction of cellular senescence and apoptosis. But how organ-specific stem cells, such as those of the adult brain, execute these antitumorigenic response mechanisms upon oncogenic stress is not well understood.

Experiments conducted both in *Drosophila* and vertebrate model systems demonstrate that NSCs are controlled by a crosstalk between mechanisms regulating self-renewal and those promoting cell-cycle exit and cellular differentiation (1). For instance, while cyclin/CDK complexes actively stimulate cells to progress through the cell cycle, in part by inactivating the cell-cycle inhibitor RB, these complexes are negatively regulated by CDK inhibitors and the p53 protein (2, 3). Apart from their roles in regulating self-renewal and differentiation under normal conditions, p53 and CDK inhibitors are rapidly activated in response to various forms of cellular stresses, such as oncogene-based pressure, and are essential for counteracting malignant transformation through the induction of cell-cycle arrest, cellular senescence, or apoptotic cell death (4–6). However, how these tumor suppressors are activated in NSCs of the adult brain to prevent oncogenic transformation and the propagation of malignant cells is not fully understood.

The HMG-box SOX transcription factor family members SOX5, SOX6, and SOX21 (SOX5/6/21) are widely expressed in NSCs of the CNS (7–12) and when overexpressed can promote embryonic NSCs to exit the cell cycle and commit to differentiation (13, 14). Interestingly, a common feature of these SOX transcription factors is their capability to counteract tumor cell expansion, as *in vitro* experiments have shown that forced expression of SOX5 and SOX21 decreases the viability of human glioma cell lines (15, 16). Although SOX6 has not been reported to alter the self-renewal of brain tumor cells, cell culture–based studies have shown that overexpression of SOX6 can suppress the expansion of non-CNS tumor cell lines (17–19). Despite these overexpression studies suggesting that SOX5/6/21 can counteract cancer cell propagation, the question whether these transcription factors can also prevent malignant transformation of NSCs in the brain, has yet to be addressed.

[1]Ludwig Institute for Cancer Research, Stockholm, Sweden. [2]Department of Cell and Molecular Biology, Karolinska Institutet, Stockholm, Sweden. [3]Department of Clinical Sciences Lund, Glioma Immunotherapy Group, Division of Neurosurgery, Lund University, Lund, Sweden. [4]Department of Oncology-Pathology, Karolinska Institutet, Stockholm, Sweden. [5]Department of Cellular and Molecular Medicine, Cleveland Clinic Lerner Research Institute, Cleveland, Ohio. [6]Department of Neurosurgery, Karolinska University Hospital, Stockholm, Sweden.

Note: Supplementary data for this article are available at Cancer Research Online (http://cancerres.aacrjournals.org/).

I. Kurtsdotter and D. Topcic contributed equally to this article.

Corresponding Author: Jonas Muhr, Ludwig Institute for Cancer Research, Nobels vag 3, Stockholm SE17177, Sweden. Phone: 467-0680-5017; Fax: 468-332-812; E-mail: jonas.muhr@ki.se

doi: 10.1158/0008-5472.CAN-17-0704

Here we have examined the role of SOX5/6/21 in NSCs of the adult mouse subventricular zone (SVZ) upon oncogenic stress. We show that SOX5/6/21 are necessary for SVZ cells to induce an antitumorigenic response to oncogenes and that the susceptibility of these cells to initiate the formation of glioma-like tumors is strongly increased by the individual or combined removal of the *Sox5/6/21* genes.

Materials and Methods

Generation of mutant mice and tumor induction

All animal procedures and experiments were performed in accordance with Swedish animal welfare laws authorized by the Stockholm Animal Ethics Committee: Dnr N249/14. Generation of $Sox5^{flox/flox}$ and $Sox6^{flox/flox}$ mice has been described previously (20, 21). C57BL/6J mice were used as wild-type controls. For lentiviral injections, 10- to 20-week-old mice were used for the experiments. Animals received stereotactially guided injections over 3 to 5 minutes into the SVZ (1.5 mm lateral and 0.6 mm anterior to bregma; depth 1.5 mm from dura) of 2 μL virus mix of HRAS, AKT, and CRE. Mice were sacrificed up to 6 months after viral injections. For transplantation of human GBM cells, NOD.CB17-PrkcSCID/J mice of 6 to 10 weeks of age were used. A total of 100,000 cells were transplanted stereotactically into striatum (2.0 mm lateral and 1.0 mm anterior to bregma; depth 2.5 mm from dura). Mice were sacrificed 3 months posttransplantation. Tumor size was calculated as an arbitrary value of GFP area at the same anterior–posterior level of multiple animals, using ImageJ.

Cell culture

Glioblastoma tissue specimens were collected via surgical resection under the ethical permit KI 02-254 (22) or 2013/576-31, issued by the Ethical Review Board at Karolinska Institutet, in accordance with the declaration of Helsinki. All samples were obtained following a written patient consent. A neuropathologist diagnosed all tissue samples collected. Primary glioblastoma cell cultures were established from fresh tumor tissue using papain (Worthington) following manufacturer's protocol, or obtained from collaborators. Cells were cultured on poly-L-ornithine and Laminin (Sigma-Aldrich) coated plates in Human NeuroCult NS-A Proliferation media (Stem Cell Technology) supplemented with 2 μg/mL heparin (Stem Cell Technology), 10 ng/mL FGF (Stem Cell Technology), 20 ng/mL EGF (Stem Cell Technology), and penicillin/streptomycin (Gibco). All primary cells were used below passage 15. U87 cell line, purchased from ATCC 2013, was cultured in DMEM containing glucose and glutamine (GIBCO), supplemented with 10 % FBS (Stem Cell Technology) and 100 μg/mL Penstrep (GIBCO). U87 cell line was used between passages 5 and 10 (from arrival in the lab) and has not been authenticated since purchase. Cells from the adult mouse SVZ were collected as previously described (23) and tissue was dissociated using papain (Worthington) following manufacturer's instructions. SVZ cells were cultured in mouse NeuroCult NS-A Proliferation media (Stem Cell Technology) according to manufacturer's protocol. Neurospheres were maintained in ultra-low attachment surface plates (Corning). All cell cultures were regularly tested for mycoplasma with MycoAlert luciferase assay (Lonza), whereby the last set of assays was performed in September of 2016.

Neurosphere-forming assays

Neurosphere formation capacity assay was conducted as previously described (24) and neurospheres subjected to size measurement using publicly available ImageJ software.

Lentiviral vectors and virus production

Lentivirus vectors pTOMO AKT and pTOMO H-RasV12 were a kind gift from Inder M. Verma (Salk Institute, La Jolla, CA). pBOB-CAG-iCRE-SD was purchased from Addgene and pLenti-GIII-CMV-hCDKN1A-GFP-2A-Puro, pLenti-GIII-CMV-hCDKN1B-GFP-2A-Puro, pLenti-GIII-CMV-hTP53-GFP-2A-Puro were obtained from Applied Biological Materials (ABM) Inc., whereas lentivirus vectors pLOC-Sox5 IRES GFP, pLOC-Sox6 IRES GFP, and pLOC-Sox21 IRES GFP were acquired from Thermo Fisher Scientific. As tranduction control, either pLOC-RFP IRES GFP or pRRLsin.PPT.CMV.ires.eGFP.pre, a kind gift from Silvia K. Nicolis (University of Milano-Bicocca, Milan, Italy), were used. Viruses were packaged in 293FT cells with either second- or third-generation packaging systems.

Lentiviral transductions and plasmid transfections

Lentiviral transductions of cells were performed at a MOI of 1–2. Transduced cells were kept in culture for 3 days (proliferation assay), 3 to 9 days (senescence assay and Western blot analysis), and 9–12 days (AnnexinV assay), before being subjected to an assay of interest. Transfection of GBM cells was conducted using the NEON transfection system (Thermo Fisher Scientific), following manufactures protocol. Transfected cells were kept in culture for 3 days, before undergoing a proliferation assay.

Proliferation, senescence, and cell death assays

For proliferation assays cultured cells were pulsed with 10 μmol/L ethynyldeoxyuridine (EdU; Molecular Probes) for 1 to 2 hours and then processed for either immunohistochemistry or FACS analysis (BD FACSCantoII, BD Biosciences). EdU was visualized for manual scoring with Click-iT EdU Imaging Kit, and for FACS analysis with Click-iT EdU Flow Cytometry Assay Kit (Molecular Probes), following manufacturer's protocol. For analysis of cellular senescence, Abcam Senescence Detection Kit was used to detect X-gal–positive cells, following manufacturer's instructions. Images were acquired and color intensity was scored using ImageJ and corrected against total cell number. For analysis of cellular apoptosis, cells were processed with the APC Annexin V Apoptosis Detection Kit (BD Biosciences).

Cycloheximide chase

Cycloheximide (100 μg/mL; Sigma-Aldrich) was added to the cells 4 to 5 days after the transduction with the indicated combination of lentiviruses. Protein levels of p53 were determined by collecting cell lysates at indicated time points and performing immunoblotting as described in Supplementary Materials and Methods.

RNA isolation and qRT-PCR

RNA was isolated from transduced primary glioblastoma cells 4–5 days posttransduction using RNeasy Micro Kit (Qiagen). The RNA was used for complementary DNA synthesis with Oligo (dT) 12 to 19 (Life Technologies) using SuperScriptII Reverse Transcriptase (Life Technologies). Quantitative reverse transcriptase

PCR reactions were prepared using KAPA SYBRFAST (Kapa Biosystems).

Accession numbers

The NCBI Sequence Read Archive accession number for the sequencing data reported in this article is SRP109992.

Statistical analyses

Statistical analyses were performed when appropriate and *P* values indicated by an asterisk in the figure legends. Significant differences between means for single comparisons were determined via Student *t* test. Multiple comparison analyses were conducted using ANOVA, followed by Bonferroni correction for *post hoc* analysis. NS stands for not significant.

Additional description of Materials and Methods can be found in the Supplementary Material.

Results

SOX5/6/21 expression is increased in brain NSCs upon oncogenic stimuli

To address the role of SOX5/6/21 in brain NSCs upon oncogenic stress, we first defined their expression pattern and activity in NSCs of the adult mouse SVZ, which have been shown to be susceptible to oncogenic transformation (24–26). In this region of the brain, a vast majority of the SOX2$^+$ and NESTIN$^+$ progenitor cells expressed SOX5/6/21, and their expression could be detected in most self-renewing KI67$^+$ cells (Fig. 1A–K). Overexpression of SOX5/6/21 promotes cell-cycle exit of embryonic NSCs (Supplementary Fig. S1A and S1B; refs. 13, 14). To examine whether this function is conserved in the adult brain, SVZ cells were isolated and transduced with lentiviruses expressing GFP or SOX5/6/21 (Fig. 1L). Consistent with their function in embryonic cells, the fraction of adult NSCs that were labeled by a 1 hour pulse of EdU, 72 hours posttransduction, was reduced to less than half that of NSCs expressing GFP only (Fig. 1M).

The finding that high levels of SOX5/6/21 possess the capacity to reduce cell proliferation prompted us to examine their expression levels in adult NSCs in response to oncogenic stimuli. To address this, SVZ cells were isolated (Fig. 1L) and transduced with lentiviruses expressing CRE enzyme, with or without CRE/*loxP*-controlled lentiviruses expressing the oncogenic forms of AKT and H-RAS (AKT, H-RAS, and CRE, hereafter referred to as ARC; Fig. 1N; Supplementary Fig. S1C), which have been shown to induce a malignant phenotype in the mouse brain (25). Interestingly, while the expression levels of the general NSC markers SOX2 and NESTIN remained unchanged following ARC-transduction, the levels of SOX5/6/21 proteins were increased 5 to 7-fold in comparison with cells expressing the CRE-enzyme only (Fig. 1O and P).

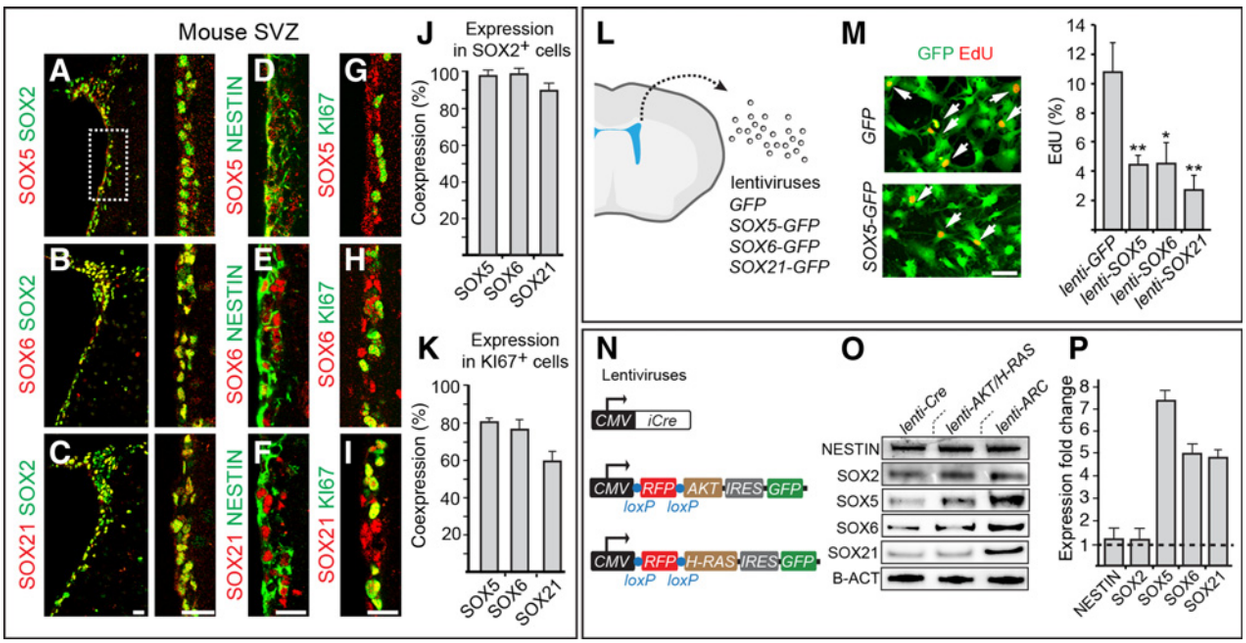

Figure 1.

SOX5/6/21 expression in the SVZ is increased by oncogenic stimuli. **A–I**, Coexpression of SOX5/6/21 (red; **A–I**) with the progenitor markers SOX2 (green; **A–C**), NESTIN (green; **D–F**), and KI67 (green; **G–I**) in the mouse SVZ. **J** and **K,** Graphs show percentage of SOX2$^+$ cells (**J**) and KI67$^+$ cells (**K**) expressing SOX5/6/21 in NSCs of the adult SVZ ($n = 6$–7 and $n = 3$ sections, respectively). **L** and **M,** Proliferation of SOX5/6/21-transduced SVZ cells was quantified as the percentage of GFP-positive cells labeled with EdU ($n = 5$–6). **N–P,** Immunoblots showing NESTIN and SOX protein levels in cultured mouse SVZ cells (**O**) after transduction with lentiviruses expressing the oncogenes AKT1 and H-RAS in a CRE-dependent manner ($n = 3$). Bar graph (**P**) shows fold-change expression of lenti-ARC over lenti-CRE and dotted line indicates a fold change of one. Scale bars in **A–I**, 20 μm; **M**, 50 μm. For all graphs, data are shown as mean ± SEM. *, $P < 0.05$; **, $P < 0.01$.

Deletion of *Sox5/6/21* potentiates the formation of glioma-like tumors

The antiproliferative activity of SOX5/6/21 and the observation that their expression levels were increased in NSCs transduced with ARC-expressing lentiviruses, raise the possibility that these proteins may be part of a cellular response mechanism, which counteracts oncogenic transformation of NSCs. To examine this possibility, we analyzed how the tumor-inducing capacity of AKT and H-RAS, in NSCs of the adult brain was affected by the loss of SOX5/6/21 expression. Lentiviruses expressing ARC (Fig. 1N) were injected into the SVZ (Fig. 2A) of adult wild-type (*Wt*) mice or mice conditionally mutant for *Sox5* (20), *Sox6* (21), or *Sox21* (see Supplementary Materials and Methods), as well as into mice harboring various combinations of these mutations. Apart from efficiently activating AKT and H-RAS expression from the CRE/*loxP*-controlled vectors (Fig. 2B–D), the virally expressed CRE-enzyme also successfully reduced SOX5/6/21 expression in the transduced SVZ cells (Fig. 2E and F; Supplementary Fig. S2A). In accordance with previous observations (25), the majority of the *Wt* brains showed no tumor formation, or only the development of minor hyperplasia, 4 to 5 months after ARC misexpression (Fig. 2G; Supplementary Table S1), and tumor formation could only be detected in approximately 15% of the treated *Wt* animals. In contrast, misexpression of ARC in mice conditionally mutant for *Sox5*, *Sox6*, or *Sox21*, or for combinations of these genes, lead to tumor formation in around 60% to 80% of the transduced brains (Supplementary Table S1). Moreover, as determined with GFP-expression, as well as with hematoxylin and eosin (H&E) staining, the tumors were significantly larger in brains of the combinatorial mutants, compared with tumors generated in the individual mutants, with the largest tumors detected in *Sox5/6/21*–mutant mice (Fig. 2G–O). Importantly, in the absence of oncogene expression, a CRE-based excision of *Sox5/6/21* did not lead to any tumor formation 5 months after the injection of CRE-expressing lentivirus (Supplementary Fig. S2B–S2I). Also, the additive effect that combinatorial loss of *Sox5/6/21* had on tumor growth indicates that these SOX proteins have partly overlapping activities. Consistent with this, tumor formation in ARC-transduced *Sox5/6*- or *Sox21*-mutant mice could be prevented by the coinjection of SOX21- and SOX6-expressing lentiviruses, respectively (Supplementary Fig. S2J–S2M). Thus, although the deletion of *Sox5/6/21* does not lead to any detectable growth anomalies, these loss-of-function experiments demonstrate that SOX5/6/21 possess overlapping activities in preventing oncogene-induced tumor formation in the SVZ.

Examination of H&E-stained tumor sections revealed characteristics typical of human high-grade gliomas, including increased cellular density, hemorrhage, cellular atypia, and microvascular proliferation (Fig. 2P–T; ref. 25). These features were most abundant in those tumors generated in combinatorial *Sox5/6/21*–mutant mice, and to a lesser extent in tumors of mice mutant for *Sox5/6* or *Sox21*. Oncogenic H-RAS and AKT have previously been demonstrated to induce astrocytic gliomas (27). In accordance, apart from expressing the NSC marker NESTIN, the tumors generated in *Sox5/6/21*–mutant mice were also highly positive for the astrocytic markers VIMENTIN and GFAP (Fig. 2U–W). However, the tumors also expressed high levels of the oligodendrocyte precursor markers PDGFRA and NG2 (Fig. 2X and Y). Similar composition of markers was found in tumors generated in the brains of *Wt* animals (Supplementary Figs. S2N–S2R), independent of the loss of the *Sox5/6/21* genes.

Loss of *Sox5/6/21* deregulates genes promoting tumor proliferation

To examine how the loss of SOX5/6/21 expression facilitates oncogenic transformation of NSCs, SVZ cells of *Wt* mice or mice conditionally mutant for *Sox5/6*, *Sox21*, or *Sox5/6/21* were isolated and characterized in neurosphere-forming assays, 2 weeks after injection of lentiviruses expressing ARC. Compared with cells from *Wt* mice, cells isolated from *Sox5/6*-, *Sox21*-, and *Sox5/6/21*–mutant mice generated a significantly higher number of neurospheres per ARC-expressing cell, with *Sox5/6/21*–mutant cells exhibiting the highest sphere-forming capacity (Fig. 3A–E). Moreover, while we could not detect any significant increase in the volume of the neurospheres generated by *Sox5/6*–mutant cells, compared with those generated by *Wt* cells transduced with ARC-expressing lentiviruses, the loss of SOX21 expression, or SOX5/6/21 expression, increased the volume of the neurospheres over two and seven times, respectively (Fig. 3A–D and F). In agreement with these observations, the fraction of $DAPI^+$ or $KI67^+$ ARC-expressing cells that incorporated EdU during a 1-hour pulse, was increased more than 30% in *Sox21*-mutant neurospheres and more than 60% in *Sox5/6/21*–mutant neurospheres, compared with *Wt* or *Sox5/6*–mutant neurospheres (Fig. 3G–K). Thus, the proliferative capacity of oncogene expressing SVZ cells is substantially increased upon the loss of *Sox5/6/21*.

Next, we used RNA-seq analysis to assess how the loss of *Sox5/6/21* affects the gene expression profile of ARC-expressing SVZ cells. In comparison to *Wt* cells transduced with ARC-expressing lentiviruses, the loss of SOX5/6/21 expression lead to an upregulation (>1.5-fold) of 993 genes and a downregulation (>1.5-fold) of 998 genes. Consistent with the findings above, gene ontology (GO) analysis of the deregulated genes revealed a significant upregulation of proliferation-associated genes, resulting in high enrichment of GO-terms such as "Mitotic cell cycle," "Cell division," and "RB in cancer" (Fig. 3L). In contrast, analysis of the downregulated genes resulted in a strong enrichment of GO-terms associated with cellular differentiation, such as "Neurogenesis," "Gliogenesis," and "Axon guidance pathway" (Fig. 3M). Interestingly, of the genes upregulated both in ARC-expressing *Sox5/6/21* mutant cells and in human GBM compared to low-grade glioma (28), we detected many genes implicated in cell-cycle regulation and tumorigenesis (e.g., *AURKA*, *FOXM1*, *E2F8*, *MELK*, *PLK1*, *BIRC5*; Fig. 3N; Supplementary Table S2; refs. 29–33). In contrast, among the genes commonly downregulated in these different cell types, we detected several genes with relevant roles in neuronal differentiation and tumor suppression (e.g., *EBF4*, *DLL1-2*, *PTCH1*, *NF1*, *FAT1*, *APC*, *BAI1*; Fig. 3O; Supplementary Table S2; refs. 34–40). Hence, *Sox5/6/21* appear to prevent oncogene-expressing SVZ cells from upregulating pro-proliferative genes that are highly expressed in human GBM.

Antitumorigenic responses by SVZ cells require SOX5/6/21

Components of the cyclin–CDK–RB axis are important regulators of tumor proliferation. Although cyclin/CDK complexes promote proliferation by inactivating the tumor suppressor protein RB (41), CDK inhibitors block this activity, and thus counteract proliferation (3). As revealed by immunoblotting, in

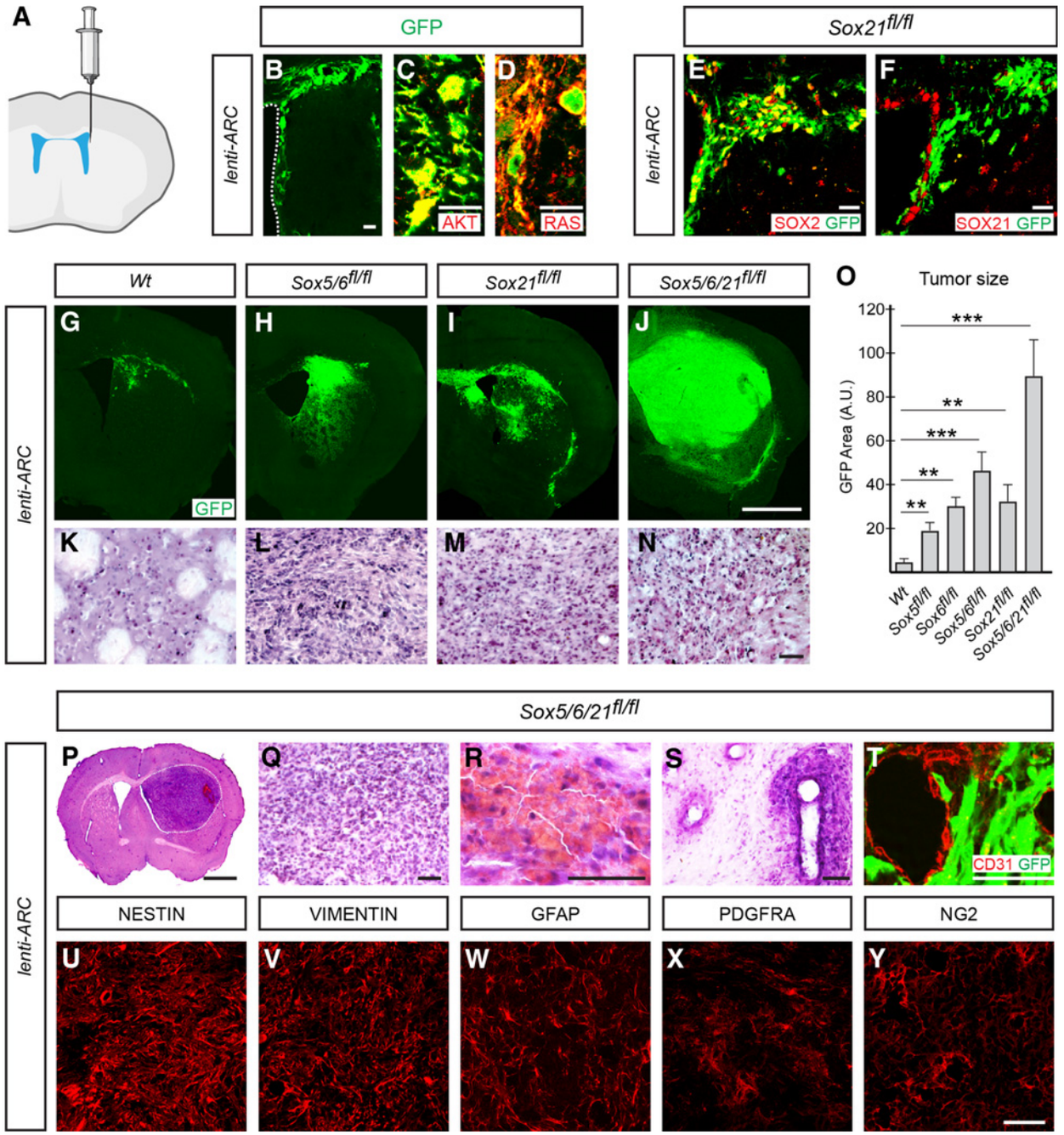

Figure 2.

Oncogene-driven transformation of SVZ cells lacking SOX5/6/21. **A–D,** Injection of ARC-expressing lentiviruses (Fig. 1N) into the adult mouse SVZ (**A**) results in the expression of GFP (**B–D**; green), AKT-HA (**C**; red), and H-RAS-Flag (**D**; red). **E** and **F,** Two weeks after injection of ARC-expressing lentiviruses, transduced cells express normal levels of SOX2 (**E**; red), but only low levels of SOX21 (**F**; red). **G–O,** GFP expression in tumors (**G–J**; green) and their cellular density visualized by H&E (**K–N**).**O,** Tumor size based on GFP-positive area at the same rostro-caudal level (n = 8–10 sections in 5–10 tumors). **P–T,** ARC-induced tumors in *Sox5/6/21*$^{fl/fl}$ animals analyzed with H&E. High cellular density (**Q**), bleedings (**R**), and large dilated vessels (**S**) are shown. CD31^{+} vascular endothelial cells within the GFP^{+} tumor mass (**T**). **U–Y,** NESTIN, VIMENTIN, GFAP, PDGFRA, and NG2 expression in ARC-induced tumors in *Sox5/6/21*$^{fl/fl}$ mice. Scale bars in **B–F**, 20 μm; **K–N**, **Q–T**, **U–Y**, 50 μm; **G–J**, **P**, 1 mm. For all graphs, data are shown as mean ± SEM. **, $P < 0.01$; ***, $P < 0.001$.

the absence of oncogenes, the loss of *Sox5/6/21* did not significantly alter the protein levels of cyclin D1, -D2, -E1, or -A1 in cultured SVZ cells (Supplementary Fig. S3A). However, in the presence of AKT and H-RAS expression, the loss of *Sox5/6/21* lead to a dramatic increase in cyclin levels (Fig. 4A). Cells expressing ARC responded differently to the loss of *Sox5*, *Sox6*,

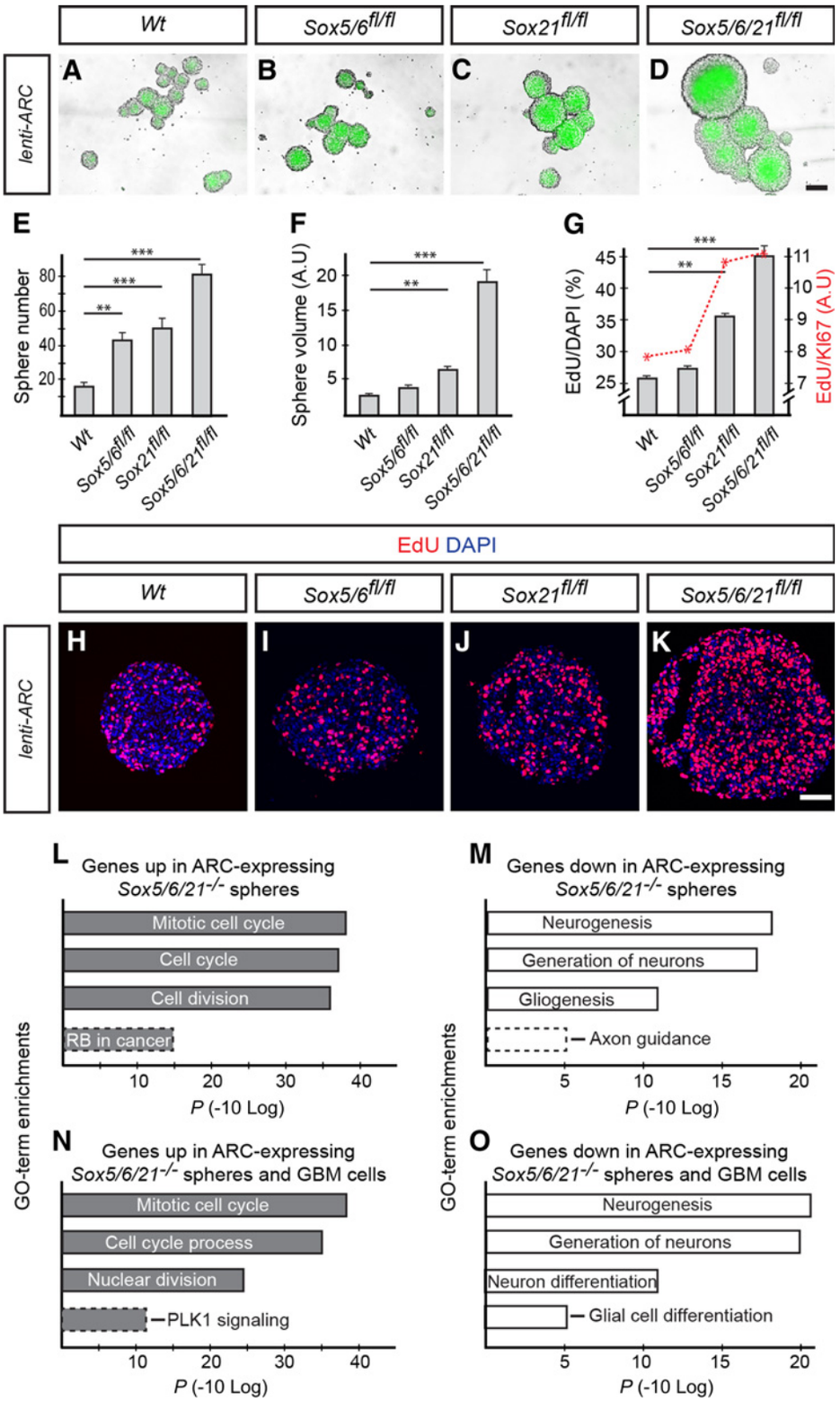

Figure 3.
SOX5/6/21 suppress genes promoting tumor proliferation. **A–K,** Neurosphere forming capacity and proliferation of SVZ cells isolated from mouse brains 2 weeks after the injection of ARC-expressing lentiviruses. Sphere size (**A–D**) and proliferation (**H–K**) were measured after 10 to 14 days of culture. **E–G,** Quantifications of formed neurospheres (**E**; $n = 6$), sphere volume (**F**; $n = 17$–22 neurospheres/group) and proliferation (**G**; $n = 5$–7). **L** and **M,** GO analysis of deregulated genes in ARC-expressing neurospheres lacking *Sox5/6/21* compared with ARC-expressing *Wt* spheres. Biological processes (solid bars) and pathways (stippled bars). **N** and **O,** GO analysis of gene sets commonly deregulated in ARC-expressing neurospheres and in human high-grade glioma, compared with low-grade glioma. X-axes show significance of enrichment. Scale bars in **H**, 50 μm; **D**, 100 μm. For all graphs, data are shown as mean ± SEM. *, $P < 0.05$; **, $P < 0.01$; ***, $P < 0.001$.

and *Sox21*. Although the upregulation of cyclin D2 and cyclin E1 levels were predominately associated with the loss of *Sox21*, the most significant increase in cyclin A1 levels was detected in *Sox5/6*–mutant cells (Fig. 4A). Even though the level of total RB remained unchanged, the level of the inactive, hyperphosphorylated form of this protein (pRB) followed that of the

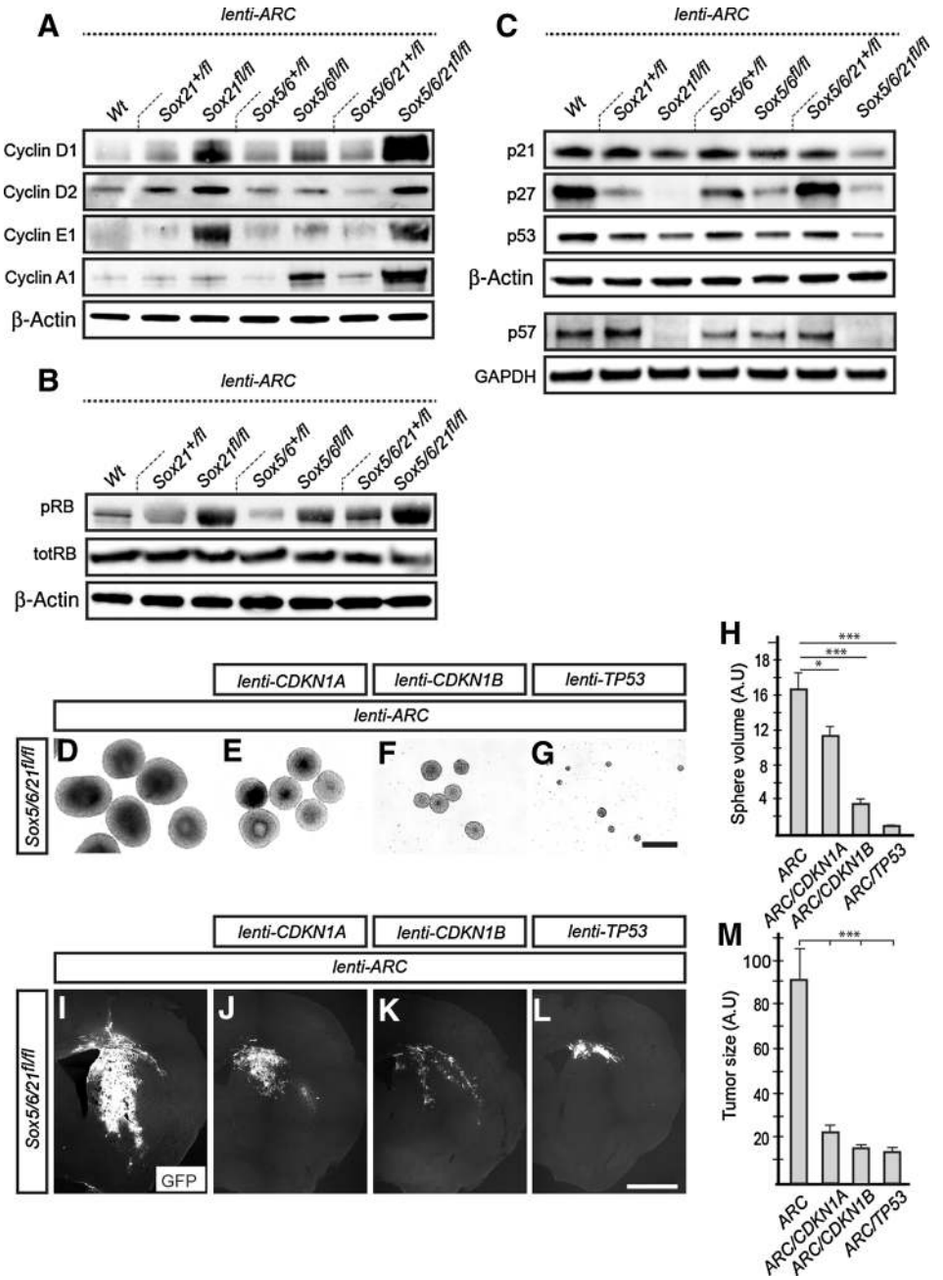

Figure 4.
SOX5/6/21 are required for tumor suppressor upregulation. **A–C**, Protein levels of cell-cycle regulatory proteins in neurospheres derived from SVZ cells of mice injected with ARC-expressing lentiviruses. **D–H,** Expression of p21 (**E**), p27 (**F**), or p53 (**G**) prevents growth of ARC-expressing SVZ-derived neurospheres (**H**; $n = 20–22$ neurospheres/group). **I–M,** *Sox5/6/21*$^{fl/fl}$ brains 1 month after the injection of ARC-expressing lentiviruses (**I**) with or without lentiviruses expressing p21 (**J**), p27 (**K**) or p53 (**L**). Quantification of tumor size as measured by GFP area (**M**; $n = 7–9$). Scale bars in **G**, 200 μm; **L**, 1 mm. For all graphs, data are shown as mean ± SEM. *, $P < 0.05$; ***, $P < 0.001$.

cyclins, and was highly increased in ARC-expressing cells mutant for *Sox5/6*, *Sox21*, and *Sox5/6/21* (Fig. 4B). In the absence of oncogene expression, the loss of *Sox5/6/21* did not lead to a significant change in pRB levels (Supplementary Fig. S3B). Moreover, although the protein levels of the CDK inhibitors p21, p27, p57, and the tumor suppressor p53 were increased in SVZ upon AKT and H-RAS expression (Supplementary Fig. S3C), this upregulation was completely abolished following the loss of *Sox5/6/21* (Fig. 4C). In the absence of oncogene expression, the lack of *Sox5/6/21* did not lead to detectable decrease in protein levels of CDK inhibitors or p53 (Supplementary Fig. S3D). Notably, a corresponding regulation of the cell-cycle regulators analyzed above could not be detected at the mRNA levels (Supplementary Table S2).

One possibility is that the inability of *Sox5/6/21* mutant SVZ cells to upregulate CDK inhibitors and p53 could explain their extensive proliferative activity and their susceptibility to malignant transformation in response to oncogenes. Consistently, restoring the expression levels of p21, p27, or p53 in *Sox5/6/21*–mutant SVZ cells transduced with ARC-expressing lentiviruses, significantly reduced their neurosphere-forming capacity (Fig. 4D–H). Moreover, lentiviral-based expression of p21, p27, or p53 substantially reduced or totally prevented ARC-induced tumor formation in *Sox5/6/21* mutant mice (Fig. 4I–M). Hence,

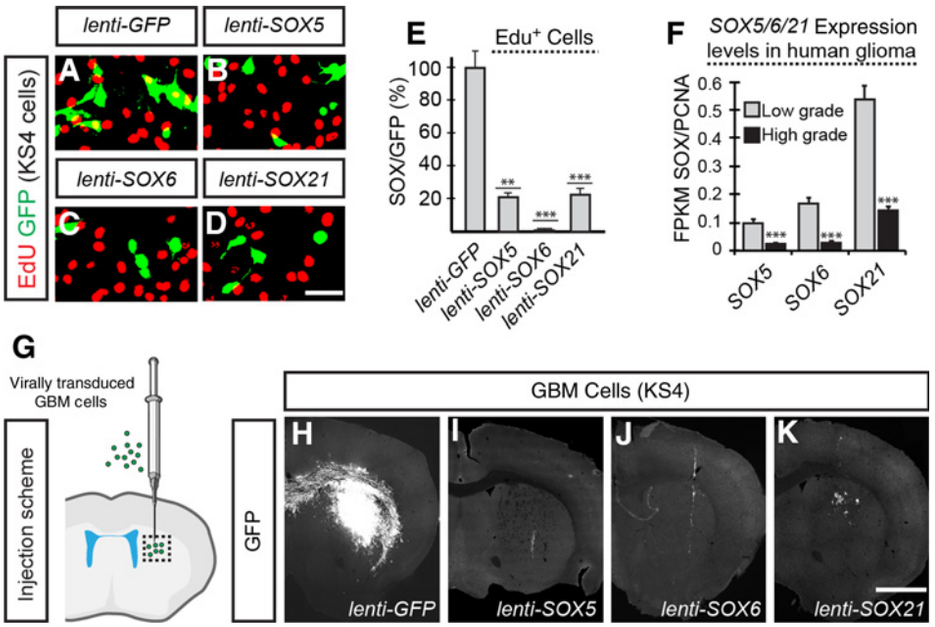

Figure 5.
High levels of SOX5/6/21 block tumor-inducing capacity of human GBM cells. **A–E,** High levels of SOX5/6/21 decrease proliferation of human GBM cells 3 days posttransduction (**A–D**). FACS-based quantification of proliferation of GBM cells overexpressing SOX5/6/21 (**E**; $n = 4$). **F,** FPKM expression levels of *SOX5/6/21*, normalized against *PCNA,* in low-grade glioma (grade II/III) and high-grade glioma (grade IV; $n = 31$–33 samples). **G–K,** Injection of human GBM cells transduced with lentiviruses expressing GFP, SOX5-GFP, SOX6-GFP, SOX21-GFP into striatum of adult NOD-SCID mice. Scale bars in **D**, 25 μm; **K**, 1 mm. For all graphs, data are shown as mean ± SEM. **, $P < 0.01$; ***, $P < 0.001$.

restoring high levels of p21, p27, and p53 blocks oncogene-induced transformation of *Sox5/6/21* mutant SVZ cells.

High SOX5/6/21 levels block tumor-inducing capacity of human GBM cells

Consistent with their capacity to counteract proliferation of mouse NSCs, forced expression of SOX5/6/21 in human primary (KS4 and G3) GBM cells or an established (U87) GBM cell line, significantly decreased the fraction of EdU incorporating cells, compared with those cells expressing GFP only (Figs. 5A–E; Supplementary Fig. S4A and S4B).

The negative relationship between SOX5/6/21 levels and GBM cell proliferation raises the question if there is a similar negative correlation between the level of *SOX5/6/21* expression and the malignancy grade in human gliomas. To address this possibility we retrieved publically available gene expression data sets of low-grade (grade II and III) and high-grade (grade IV) glioma samples analyzed with RNA-seq (28). Notably, the expression levels of SOX5/6/21 were decreased approximately four to six times in high-grade glioma samples compared to those of low-grade (Fig. 5F) and this reduction was independent of the mutational status of *TP53* in the examined glioma samples (Supplementary Fig. S4C and S4D). Consistent with these findings, although transplantation of GFP-transduced human primary GBM cells (KS4) into the striatum of NOD-SCID mice (Fig. 5G) resulted in large tumors 3 months postinjection (Fig. 5H), GBM cells mis-expressing either SOX5, SOX6, or SOX21, failed to form secondary tumors upon transplantation (Fig. 5I–K). Thus, apart from preventing mouse SVZ cells from malignant transformation, SOX5/6/21 can also reduce proliferation and the tumor-inducing capacity of human primary GBM cells.

SOX5/6/21 can restore tumor suppressor responses in human GBM cells

The fact that increased levels of SOX5/6/21 counteract proliferation of human GBM cells, both *in vitro* and *in vivo*, raises the possibility that SOX5/6/21 play a role in restoring an antitumorigenic expression profile in cancer cells that are already exhibiting a malignant profile. To address this hypothesis we analyzed the transcriptomes of five primary human GBM cell lines (KS4, G3, JM3, #87, and #89) and of the established glioma cell line U87 (42), 72 hours after transduction with SOX5/6/21-expressing lentiviruses (Supplementary Fig. S5A). The transduced cells responded to SOX5/6/21 expression by deregulating thousands of genes (>1.5-fold; Fig. 6A; Supplementary Fig. S5B). Comparisons of the up- and down-regulated genes revealed a significantly higher overlap between the genes deregulated by SOX5 and SOX6, compared with the genes deregulated by SOX21 (Fig. 6B; Supplementary Fig. S5C). GO-term analysis of genes deregulated by SOX5/6/21 in the primary and the established GBM cell lines, KS4 and U87, revealed a strong repression of proliferation-associated genes, resulting in an enrichment of GO terms, including "Mitotic cell cycle," "Nuclear division," and "RB in cancer" (Fig. 6C; Supplementary Fig. S5D). Interestingly, analysis of the genes upregulated by SOX5/6/21 instead resulted in a significant enrichment of GO terms associated with general tumor suppressor responses, including "Apoptotic process," "Cellular response to stress," "Direct p53 effector," and "Senescence and Autophagy" (Fig. 6C; Supplementary Fig. S5D).

Cellular defense mechanisms following oncogenic stress are mediated through the upregulation of CDK inhibitors and tumor suppressors, which results in the deceleration of cell-cycle progression, as well as induction of cellular senescence and apoptosis. Because p16, p21, p27, p57, and p53 are potent regulators of these cellular processes (4, 5, 43, 44), we assessed the expression levels of these proteins in cultured human primary GBM cells, 72 hours after the transduction with SOX5/6/21-expressing lentiviruses. As expected, both the primary GBM cells and the established GBM cell lines had undetectable, or only low levels of p16, p21, p27, p57, and p53 proteins (Fig. 6D). However, the levels of these proteins were significantly upregulated in the different cell lines in response to forced expression of SOX5/6/21 (Fig. 6D). Notably, even

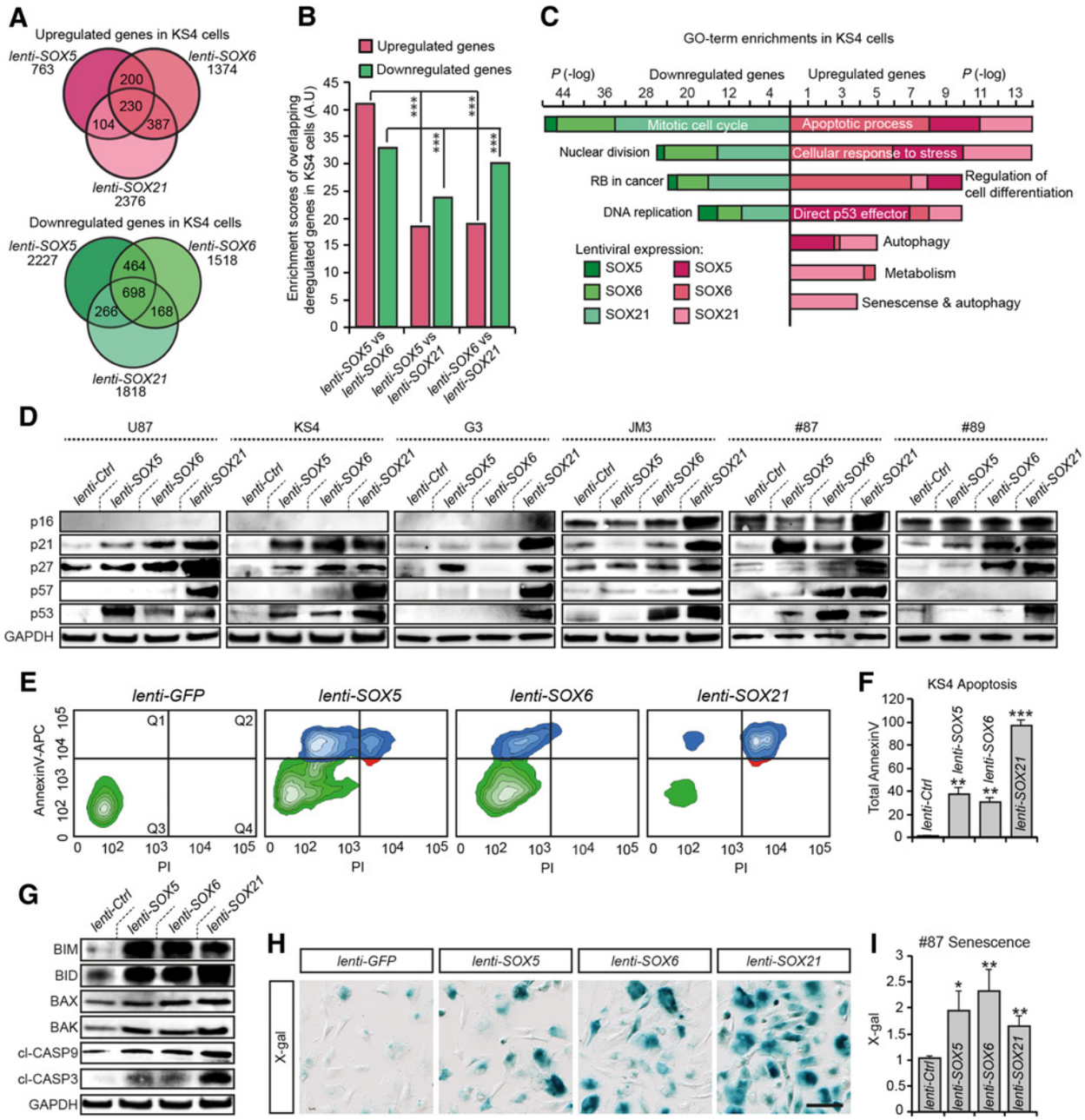

Figure 6.

SOX5/6/21 can restore tumor suppressor responses in human GBM cells. **A,** Deregulated genes in human primary GBM cells, KS4, after the transduction with SOX5-, SOX6-, or SOX21-expressing lentiviruses ($n = 3$). **B,** Gene overlap enrichment scores showing correlations of genes up- or downregulated in human primary GBM cells, KS4, after the transduction with SOX5-, SOX6-, or SOX21-expressing lentiviruses ($n = 3$). **C,** GO analysis on gene sets up- and downregulated in human primary GBM cells, KS4, transduced with SOX5/6/21-expressing lentiviruses. Significant GO terms are represented in the collapsed bars. **D,** Expression of p16, p21, p27, p57, and p53 in five human primary GBM cell samples and the glioma cell line U87 4 days after transduction with SOX5-, SOX6-, or SOX21-expressing lentiviruses. **E** and **F,** FACS-analysis of cell death 9 to 12 days after that GBM cells were transduced with SOX5/6/21 expressing lentiviruses. Quantification of total Annexin V labeling shown as fold change over GFP control (**F**; $n = 3$). Q1, early apoptotic cells; Q2, late apoptotic cells; Q3, live cells; Q4, necrotic cells. **G,** Expression of BIM, BID, BAX, BAK, and cleaved caspase-9 and -3 in SOX5/6/21–transduced human primary GBM cells (KS4). **H** and **I,** X-gal–based detection of cellular senescence in primary human GBM cells (#87) more than 3 days posttransduction with SOX5/6/21–expressing lentiviruses. Quantification of X-gal color intensity and area (**I**; $n = 8$). Scale bars in **H**, 20 μm. For all graphs, data are shown as mean ± SEM. *, $P < 0.05$; **, $P < 0.01$; ***, $P < 0.001$.

though their level of upregulation varied in a cell specific manner, cells transduced with SOX21-expressing lentiviruses exhibited the most abundant increase in the protein levels of p16, p21, p27, p57, and p53, compared to those cells overexpressing SOX5 or SOX6 (Fig. 6D).

Because the induction of apoptosis and cellular senescence has been attributed to the activity of CDK inhibitors and p53, we next examined these cellular processes in cultured human GBM cells after transduction with SOX5/6/21-expressing lentiviruses. In line with the upregulation of CDK inhibitors and p53, flow cytometry-based analysis of fluorochrome-labeled Annexin V levels revealed a significantly higher level of apoptosis in U87 cells, as well as, in the five primary GBM cell lines (KS4, G3, JM3, #87, and #89) overexpressing SOX5/6/21, compared to those cells transduced with GFP-expressing lentiviruses (Fig. 6E and F; Supplementary Fig. S5E). Consistently, forced expression of SOX5/6/21 resulted in increased levels of the pro-apoptotic proteins BIM, BID, BAX, and BAK, together with upregulation of the active forms of CASPASE-9 and -3, indicating that SOX5/6/21 proteins induce apoptosis in these human primary GBM cells through permeabilization of the mitochondrial membrane (Fig. 6G; Supplementary Fig. S5F; refs. 45, 46). Furthermore, forced expression of SOX5/6/21 significantly increased the number of cells that entered senescence in the three human primary GBM cell lines (KS4, G3, and #87), as measured by senescence-associated βgal-activity (SA-βgal) and the cleavage of X-gal (Fig. 6H and I; Supplementary Fig. S5G; ref. 15).

SOX21 mediates tumor suppressor response by modulating p53 levels

Although the above findings provide evidence that increased levels of SOX5, SOX6, and in particular SOX21, are sufficient to restore tumor suppressor responses in human primary GBM cells, shRNA-mediated knockdown of p53 expression inhibited apoptosis and cellular senescence in response to forced SOX21 expression (Fig. 7A–E). The observation that the presence of p53 protein appears to be central for the capacity of SOX21 to facilitate a tumor suppressor response in GBM cells raises the question of how SOX21 promotes the increase in p53 levels. Notably, despite a robust increase in p53 protein levels upon forced SOX21 expression (Figs. 6D and 7A and B), a corresponding upregulation of *TP53* gene expression could not be detected (Supplementary Fig. S6A). In fact, although the protein levels of CDK inhibitors (p16, p21, p27, p57) and p53 were increased in response to SOX21 overexpression (Figs. 6D and 7A and B), only *CDKN1A* (p21) and *CDKN1C* (p57) demonstrated a significant upregulation at the mRNA level (Supplementary Figs. S6B–S6E). Moreover, while *CDKN1A* expression is positively regulated by p53 protein (Fig. 7A and B; Supplementary Fig. S6F; ref. 44), the ability of SOX21 to upregulate the expression of *CDKN1A* was completely abolished in the presence of shRNA targeting *TP53* (Supplementary Fig. S6G and S6H). Consistent with these findings, ChIP-seq–based binding studies of SOX21 in human primary GBM cells (KS4) failed to detect any SOX21 binding in the vicinity of the transcriptional start (<500 kilo base-pairs) of *CDKN1A*, *-1B*, *-1C*, *-2A*, or *TP53* (Supplementary Fig. S6I; Supplementary Table S3). Thus, the ability of SOX21 to upregulate p16, p27, and p53 appears mainly to be achieved at the protein level.

We next examined if SOX21-driven upregulation of p53 is achieved through an ability to stabilize this tumor suppressor on a protein level (47). Indeed, SOX21 markedly extended the half-life of p53 protein in human primary GBM cells (#87) and the glioma cell line U87 after protein synthesis inhibition by cycloheximide (Fig. 7F and G). SOX21 misexpression in these cells also resulted in the upregulation of phosphorylated (Ser15) p53, which is a stable form of this protein (Fig. 7H and I). Moreover, the level of the ubiquitin-protein ligase, MDM2, which is a negative regulator of p53 (48), was significantly reduced in GBM cells overexpressing SOX21 (Fig. 7J and K). However, SOX21 failed to downregulate *MDM2* mRNA (Supplementary Fig. S6J) and neither could we detect any binding of SOX21 to the *MDM2* gene (Supplementary Table S3). Together these data show that SOX21 can in part restore initiation of a tumor suppressor response in GBM cells by counteracting p53 protein turnover, possibly through the regulation of MDM2 protein levels (Fig. 7L).

Discussion

Stem cells in the adult body are essential for the maintenance of organ integrity, plasticity, and homeostasis (49), but their presence also constitutes a potential risk, as stem cells are faced with the difficult task of avoiding premature cell-cycle exit and at the same time being prepared to escape uncontrolled proliferation associated with neoplasia. In this study we have examined the role of SOX5/6/21 transcription factors in preventing stem cells of the brain from transformation upon oncogenic insult. We provide evidence that SOX5/6/21 are essential for the activation of antiproliferative proteins and tumor suppressors in response to oncogenic stimuli and, consequently, that the loss of SOX5/6/21 expression in the mouse SVZ greatly potentiates the induction of tumors by AKT and H-RAS.

Gene targeting experiments have revealed a number of different roles of SOX5/6/21 in the CNS, such as regulation of oligodendrocyte differentiation (10), neuronal maturation in the adult hippocampus (7), and subtype specification of cortical interneurons and midbrain dopamine neurons (8, 50, 51). However, even though high levels of SOX5/6/21 can block NSC proliferation (13, 14), loss-of-function studies have not revealed any general role for SOX5/6/21 in regulating cell-cycle progression, neither in the developing nor the adult CNS. Moreover, in this study we failed to detect any signs of excessive proliferation in the adult SVZ when SOX5/6/21 were collectively deleted through CRE-mediated excision. In this respect, it is interesting to note the dramatic tumorigenic phenotype that is displayed in *Sox5/6/21* mutant mice under conditions of oncogenic stimuli. Thus, indicating that one of the most prominent roles of SOX5/6/21 in NSCs may only be revealed under tumorigenic conditions. In agreement with this possibility, although the increased tumor burden in ARC-injected *Sox5/6/21* mutant mice was associated with a prominent increase in expression of cyclin proteins, combined with a failure to upregulate CDK inhibitors and p53, or maintain high levels of active RB, the expression levels of these factors were not generally altered by the loss of *Sox5/6/21*, in the absence of ectopic AKT and H-RAS. Although there are several possible explanations to the context-dependent function of SOX5/6/21, it is notable that the capacity of SOX5/6/21 to induce a tumor suppressor response appears to be limited to cells exposed to oncogenic stress.

How do then SOX5/6/21 facilitate the upregulation of an antitumorigenic expression profile upon oncogenic stress? The

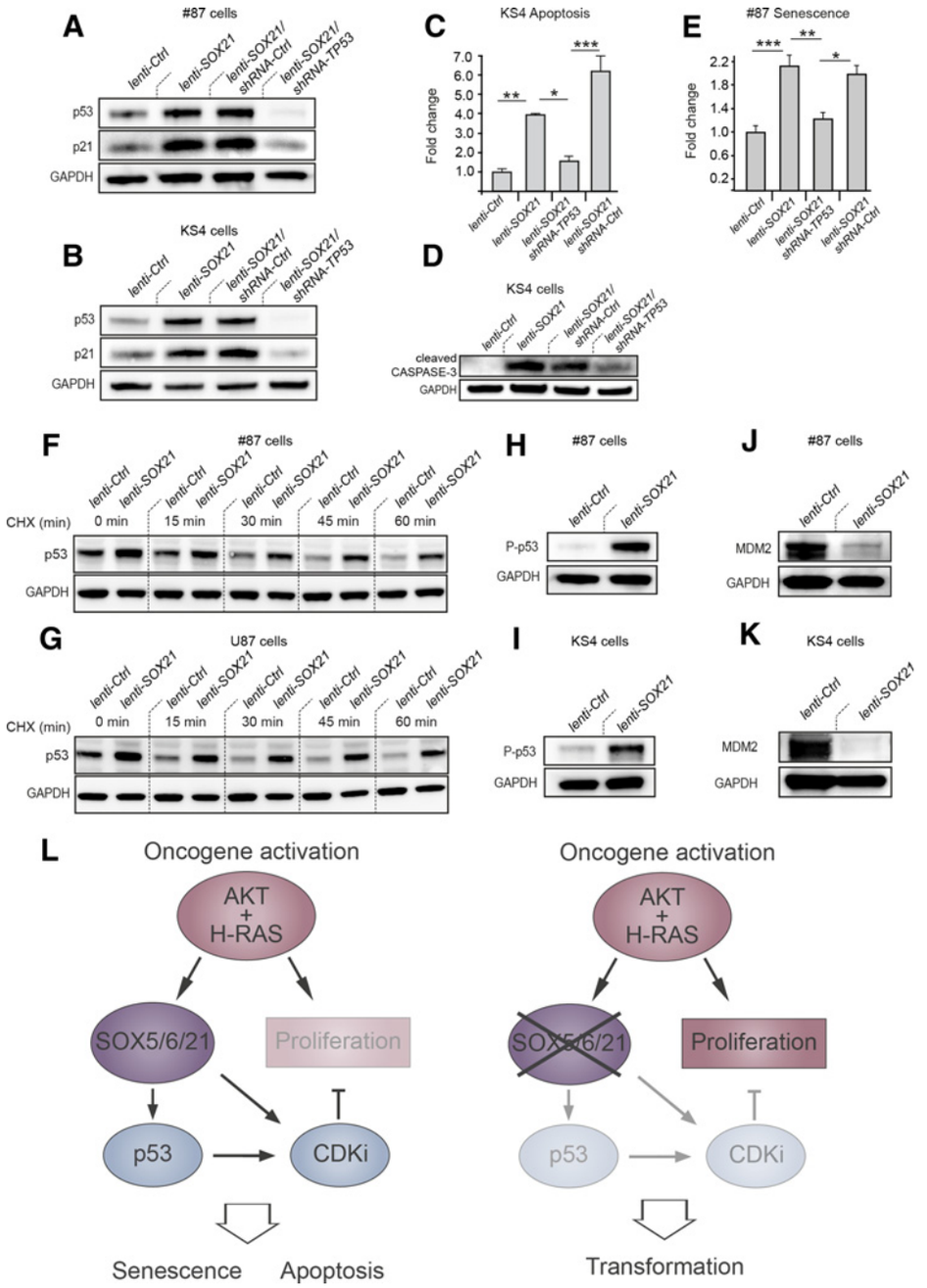

Figure 7.

SOX21 decreases p53 protein turnover. **A** and **B,** p53 and p21 protein levels in human primary GBM cells, #87 (**A**) and KS4 cells (**B**), 4 days after the transduction with lentiviruses expressing SOX21, scrambled shRNAs or shRNAs targeting *TP53* transcripts. **C,** Analysis of cell death of primary human GBM cells (KS4) 8 days after the misexpression of SOX21 with or without control shRNAs, or shRNAs targeting *TP53* transcripts ($n = 3$). **D,** Expression of cleaved caspase-3 in human primary GBM cells (KS4) 8 days after the transduction with lentiviruses expressing SOX21, control shRNAs, or shRNAs targeting *TP53* transcripts. **E,** Quantifications of X-gal–based detection of cellular senescence in human primary GBM cells (#87) as fold change over GFP control ($n = 3$). **F** and **G,** Cycloheximide (CHX)-based p53 protein turn-over assay in human primary GBM cells (#87; **F**) and U87 glioma cell line (**G**) 4 to 5 days posttransduction with control and SOX21 expressing lentiviruses. **H** and **I,** Expression of phosphorylated p53 (P-p53) in the human primary GBM cells #87 (**H**) and KS4 (**I**) transduced with SOX21 or control-expressing lentiviruses. **J** and **K,** Expression of MDM2 in human primary GBM cells (#87; **J**) and (KS4; **K**) transduced with SOX21 or control-expressing lentiviruses. **L**, Model of how Sox5/6/21 prevent oncogenic transformation. For all graphs, data are shown as mean ± SEM. *, $P < 0.05$; **, $P < 0.01$; ***, $P < 0.001$.

expression of CDK inhibitors and p53 has been shown to largely be regulated at the posttranscriptional level, through modulation of mRNA translation and protein stability (4, 5, 43, 44). Consistent with this, even though forced expression of SOX5/6/21 deregulated thousands of genes in human GBM cells, the prominent upregulation of CDK inhibitors and p53 at the protein level was only paralleled by an increased transcription of *CDKN1A* and *CDKN1C*. By analyzing how SOX21 controls the expression of p21 and p53, both at the gene regulatory and at the protein level, we have demonstrated that SOX21 fails to regulate the transcription of *TP53*, but efficiently reduces p53 protein turnover. We have also provided evidence that this function of SOX21 is necessary for its capacity to activate p21 expression, both at the transcriptional and protein level. Thus, because p53 is an efficient inducer of *CDKN1A* activity, it is reasonable to hypothesize that the transcriptional activation of p21 by SOX21 is only indirect via p53. In support of this idea, SOX21 fails to upregulate p21 mRNA and protein expression in the absence of p53. Moreover, our ChIP-seq studies in human GBM cells failed to detect any binding of SOX21 in the vicinity of the transcriptional start of *CDKN1A*. How is then SOX21 decreasing p53 protein turnover? We detected a substantial decrease in MDM2 protein levels in GBM cells transduced with SOX21-expressing lentiviruses. Hence, it is possible that the capacity of SOX21 to facilitate a tumor suppressor

response in oncogene-expressing cells, at least in part, is mediated through its ability to lower the levels of a negative regulator of p53 protein, MDM2.

We have provided evidence that SOX5/6/21 have partly overlapping activities in mediating an antitumorigenic response to oncogenic stimuli. Although individual mutations of the *Sox5/6/21* genes increased the predisposition of SVZ cells to become tumorigenic in response to oncogenes, SVZ cells in which *Sox5/6/21* were collectively deleted had the highest tumor forming capacity. Moreover, although SOX21 misexpression could prevent AKT and H-RAS-induced tumor formation in *Sox5/6* mutant mice, SOX6 misexpression could hinder tumor induction in mice mutant for *Sox21*. Studies in hepatocellular carcinoma cells have also shown that SOX6, similarly to SOX21, can decrease p53 protein turnover and that the upregulation of p21 protein by SOX6 is decreased in the presence of a p53 inhibitor (19, 47). However, SOX5/6 are more structurally related to each other, than to SOX21, and share amino acid sequence similarities both within and outside their DNA-binding HMG-domains (52). Consistently, comparing the genes and proteins deregulated in our gain- and loss-of-function experiments also revealed a substantial difference in the activity of SOX5/6 and SOX21. For instance, although cyclin D2 and -E2 levels were most upregulated in ARC-expressing SVZ cells in response to the loss of *Sox21*, the increased levels of cyclin A1 were most prominent in those oncogene-transformed cells lacking *Sox5/6*, indicating that SOX5/6/21 counteract proliferation of oncogene-expressing NSCs by regulating different phases of the cell cycle. Finally, although SOX21 is mainly expressed in precursor cells of the CNS and the gastro-intestinal tract, expression of SOX5/6 can be detected in an array of different cell types (www.proteinatlas.org; ref. 53). Thus, it is possible that SOX5/6/21 could also act in different combinations to prevent oncogenic transformation of stem cells outside the CNS.

Disclosure of Potential Conflicts of Interest

No potential conflicts of interest were disclosed.

Authors' Contributions

Conception and design: I. Kurtsdotter, D. Topcic, A. Karlén, J. Muhr
Development of methodology: I. Kurtsdotter, D. Topcic, A. Karlén, M. Nistér, V. Lefebvre, J. Muhr
Acquisition of data (provided animals, acquired and managed patients, provided facilities, etc.): I. Kurtsdotter, D. Topcic, A. Karlén, B. Singla, M. Bergsland, M. Nistér, J.W. Carlson, O. Persson
Analysis and interpretation of data (e.g., statistical analysis, biostatistics, computational analysis): I. Kurtsdotter, D. Topcic, A. Karlén, B. Singla, D.W. Hagey, M. Bergsland, J.W. Carlson, J. Muhr
Writing, review, and/or revision of the manuscript: I. Kurtsdotter, D. Topcic, M. Nistér, J.W. Carlson, J. Holmberg, J. Muhr
Administrative, technical, or material support (i.e., reporting or organizing data, constructing databases): D. Topcic, A. Karlén, B. Singla, D.W. Hagey
Study supervision: J. Muhr

Acknowledgments

We thank I. Peredo for his contribution in the establishment of human primary glioblastoma cells KS4 and G3, T. Perlmann for comments on the manuscript, and members of the Muhr labs for fruitful discussions and advice.

Grant Support

This work was supported by The Swedish Cancer Society CAN2015/781 to J. Holmberg and CAN2016/808 to J. Muhr, The Swedish Childhood Cancer Foundation NBCNS 08/017 to M. Nister, J. Holmberg, P. Siesjö, and J. Muhr, The Wallenberg Foundation KAW2012.01.01 to J. Muhr, The Swedish Research Council 2016-05307 to J. Muhr.

The costs of publication of this article were defrayed in part by the payment of page charges. This article must therefore be hereby marked *advertisement* in accordance with 18 U.S.C. Section 1734 solely to indicate this fact.

Received March 16, 2017; revised May 19, 2017; accepted June 29, 2017; published OnlineFirst July 7, 2017.

References

1. Doe CQ. Neural stem cells: balancing self-renewal with differentiation. Development 2008;135:1575–87.
2. Riley T, Sontag E, Chen P, Levine A. Transcriptional control of human p53-regulated genes. Nat Rev Mol Cell Biol 2008;9:402–12.
3. Besson A, Dowdy SF, Roberts JM. CDK inhibitors: cell cycle regulators and beyond. Dev Cell 2008;14:159–69.
4. Chu IM, Hengst L, Slingerland JM. The Cdk inhibitor p27 in human cancer: prognostic potential and relevance to anticancer therapy. Nat Rev Cancer 2008;8:253–67.
5. Bieging KT, Mello SS, Attardi LD. Unravelling mechanisms of p53-mediated tumour suppression. Nat Rev Cancer 2014;14:359–70.
6. Abbas T, Dutta A. p21 in cancer: intricate networks and multiple activities. Nat Rev Cancer 2009;9:400–14.
7. Matsuda S, Kuwako K-I, Okano HJ, Tsutsumi S, Aburatani H, Saga Y, et al. Sox21 promotes hippocampal adult neurogenesis via the transcriptional repression of the Hes5 gene. J Neurosci 2012;32:12543–57.
8. Azim E, Jabaudon D, Fame RM, Macklis JD. SOX6 controls dorsal progenitor identity and interneuron diversity during neocortical development. Nat Neurosci 2009;12:1238–47.
9. Hao H, Li Y, Tzatzalos E, Gilbert J, Zala D, Bhaumik M, et al. Identification of a transient Sox5 expressing progenitor population in the neonatal ventral forebrain by a novel cis-regulatory element. Dev Biol 2014;393:183–93.
10. Stolt CC, Schlierf A, Lommes P, Hillgärtner S, Werner T, Kosian T, et al. SoxD proteins influence multiple stages of oligodendrocyte development and modulate SoxE protein function. Dev Cell 2006;11:697–709.
11. Uchikawa M, Kamachi Y, Kondoh H. Two distinct subgroups of Group B Sox genes for transcriptional activators and repressors: their expression during embryonic organogenesis of the chicken. Mech Dev 1999;84:103–20.
12. Rex M, Uwanogho DA, Orme A, Scotting PJ, Sharpe PT. cSox21 exhibits a complex and dynamic pattern of transcription during embryonic development of the chick central nervous system. Mech Dev 1997;66:39–53.
13. Sandberg M, Källström M, Muhr J. Sox21 promotes the progression of vertebrate neurogenesis. Nat Neurosci 2005;8:995–1001.
14. Martinez-Morales PL, Quiroga AC, Barbas JA, Morales AV. SOX5 controls cell cycle progression in neural progenitors by interfering with the WNT-beta-catenin pathway. EMBO Rep 2010;11:466–72.
15. Tchougounova E, Jiang Y, Bråsäter D, Lindberg N, Kastemar M, Asplund A, et al. Sox5 can suppress platelet-derived growth factor B-induced glioma development in Ink4a-deficient mice through induction of acute cellular senescence. Oncogene 2009;28:1537–48.
16. Caglayan D, Lundin E, Kastemar M, Westermark B, Ferletta M. Sox21 inhibits glioma progression in vivo by forming complexes with Sox2 and stimulating aberrant differentiation. Int J Cancer 2013;133:1345–56.
17. Qin Y-R, Tang H, Xie F, Liu H, Zhu Y, Ai J, et al. Characterization of tumor-suppressive function of SOX6 in human esophageal squamous cell carcinoma. Clin Cancer Res 2011;17:46–55.
18. Li H, Zheng D, Zhang B, Liu L, Ou J, Chen W, et al. Mir-208 promotes cell proliferation by repressing SOX6 expression in human esophageal squamous cell carcinoma. J Transl Med 2014;12:196.
19. Xie Q, Chen X, Lu F, Zhang T, Hao M, Wang Y, et al. Aberrant expression of microRNA 155 may accelerate cell proliferation by targeting sex-

determining region Y box 6 in hepatocellular carcinoma. Cancer 2012; 118:2431–42.
20. Dy P, Han Y, Lefebvre V. Generation of mice harboring a Sox5 conditional null allele. Genesis 2008;46:294–9.
21. Dumitriu B, Dy P, Smits P, Lefebvre V. Generation of mice harboring a Sox6 conditional null allele. Genesis 2006;44:219–24.
22. Holmberg J, He X, Peredo I, Orrego A, Hesselager G, Ericsson C, et al. Activation of neural and pluripotent stem cell signatures correlates with increased malignancy in human glioma. PLoS ONE 2011;6:e18454.
23. Doetsch F, Caillé I, Lim DA, García-Verdugo JM, Alvarez-Buylla A. Subventricular zone astrocytes are neural stem cells in the adult mammalian brain. Cell 1999;97:703–16.
24. Alcantara Llaguno S, Chen J, Kwon C-H, Jackson EL, Li Y, Burns DK, et al. Malignant astrocytomas originate from neural stem/progenitor cells in a somatic tumor suppressor mouse model. Cancer Cell 2009; 15:45–56.
25. Marumoto T, Tashiro A, Friedmann-Morvinski D, Scadeng M, Soda Y, Gage FH, et al. Development of a novel mouse glioma model using lentiviral vectors. Nat Med 2009;15:110–6.
26. Jackson EL, Alvarez-Buylla A. Characterization of adult neural stem cells and their relation to brain tumors. Cells Tissues Organs 2008;188: 212–24.
27. Lindberg N, Jiang Y, Xie Y, Bolouri H, Kastemar M, Olofsson T, et al. Oncogenic signaling is dominant to cell of origin and dictates astrocytic or oligodendroglial tumor development from oligodendrocyte precursor cells. J Neurosci 2014;34:14644–51.
28. Cancer Genome Atlas Research Network. Comprehensive genomic characterization defines human glioblastoma genes and core pathways. Nature 2008;455:1061–8.
29. Dominguez-Brauer C, Thu KL, Mason JM, Blaser H, Bray MR, Mak TW. Targeting mitosis in cancer: emerging strategies. Mol Cell 2015;60:524–36.
30. Altieri DC. Survivin: the inconvenient IAP. Semin Cell Dev Biol 2015; 39:91–6.
31. Chen H-Z, Tsai S-Y, Leone G. Emerging roles of E2Fs in cancer: an exit from cell cycle control. Nat Rev Cancer 2009;9:785–97.
32. Joshi K, Banasavadi-Siddegowda Y, Mo X, Kim S-H, Mao P, Kig C, et al. MELK-dependent FOXM1 phosphorylation is essential for proliferation of glioma stem cells. Stem Cells 2013;31:1051–63.
33. Ganguly R, Hong CS, Smith LGF, Kornblum HI, Nakano I. Maternal embryonic leucine zipper kinase: key kinase for stem cell phenotype in glioma and other cancers. Mol Cancer Ther 2014;13:1393–8.
34. Briggs KJ, Corcoran-Schwartz IM, Zhang W, Harcke T, Devereux WL, Baylin SB, et al. Cooperation between the Hic1 and Ptch1 tumor suppressors in medulloblastoma. Genes Dev 2008;22:770–85.
35. Ratner N, Miller SJ. A RASopathy gene commonly mutated in cancer: the neurofibromatosis type 1 tumour suppressor. Nat Rev Cancer 2015;15: 290–301.
36. Morris LGT, Kaufman AM, Gong Y, Ramaswami D, Walsh LA, Turcan §, et al. Recurrent somatic mutation of FAT1 in multiple human cancers leads to aberrant Wnt activation. Nat Genet 2013;45:253–61.
37. Aoki K, Taketo MM. Adenomatous polyposis coli (APC): a multi-functional tumor suppressor gene. J Cell Sci 2007;120:3327–35.
38. Zhu D, Hunter SB, Vertino PM, Van Meir EG. Overexpression of MBD2 in glioblastoma maintains epigenetic silencing and inhibits the antiangiogenic function of the tumor suppressor gene BAI1. Cancer Res 2011;71: 5859–70.
39. Liao D. Emerging roles of the EBF family of transcription factors in tumor suppression. Mol Cancer Res 2009;7:1893–901.
40. Kawaguchi D, Yoshimatsu T, Hozumi K, Gotoh Y. Selection of differentiating cells by different levels of delta-like 1 among neural precursor cells in the developing mouse telencephalon. Development 2008;135: 3849–58.
41. Lanigan F, Geraghty JG, Bracken AP. Transcriptional regulation of cellular senescence. Oncogene 2011;30:2901–11.
42. Clark MJ, Homer N, O'Connor BD, Chen Z, Eskin A, Lee H, et al. U87MG decoded: the genomic sequence of a cytogenetically aberrant human cancer cell line. PLoS Genet; 2010;6:e1000832.
43. LaPak KM, Burd CE. The molecular balancing act of p16(INK4a) in cancer and aging. Mol Cancer Res 2014;12:167–83.
44. Jung Y-S, Qian Y, Chen X. Examination of the expanding pathways for the regulation of p21 expression and activity. Cell Signal 2010;22:1003–12.
45. Dewson G, Kluck RM. Mechanisms by which Bak and Bax permeabilise mitochondria during apoptosis. J Cell Sci 2009;122:2801–8.
46. Bhola PD, Letai A. Mitochondria—judges and executioners of cell death sentences. Mol Cell 2016;61:695–704.
47. Wang J, Ding S, Duan Z, Xie Q, Zhang T, Zhang X, et al. Role of p14ARF-HDM2-p53 axis in SOX6-mediated tumor suppression. Oncogene 2016; 35:1692–702.
48. Oliner JD, Saiki AY, Caenepeel S. The role of MDM2 amplification and overexpression in tumorigenesis. Cold Spring Harb Perspect Med 2016;6: a026336.
49. Ming G-L, Song H. Adult neurogenesis in the mammalian central nervous system. Annu Rev Neurosci 2005;28:223–50.
50. Lai T, Jabaudon D, Molyneaux BJ, Azim E, Arlotta P, Menezes JRL, et al. SOX5 controls the sequential generation of distinct corticofugal neuron subtypes. Neuron 2008;57:232–47.
51. Panman L, Papathanou M, Laguna A, Oosterveen T, Volakakis N, Acampora D, et al. Sox6 and Otx2 control the specification of substantia nigra and ventral tegmental area dopamine neurons. Cell Rep 2014;8:1018–25.
52. Guth SIE, Wegner M. Having it both ways: Sox protein function between conservation and innovation. Cell Mol Life Sci 2008;65:3000–18.
53. Uhlén M, Fagerberg L, Hallström BM, Lindskog C, Oksvold P, Mardinoglu A, et al. Proteomics. Tissue-based map of the human proteome. Science 2015;347:1260419–9.